

BEAM OPTICS DESIGN FOR PAL-XFEL*

H. S. Kang[†], J.-H. Han, T. H. Kang, I. S. Ko,
 Pohang Accelerator Laboratory, POSTECH, Pohang 790-784, Korea

Abstract

The PAL-XFEL lattice is designed to generate a 0.1 nm hard X-ray FEL using a 10 GeV electron linac with a switch line at 3 GeV point for 1-3 nm soft X-ray FEL. The beam optics is designed so as to have robustness in matching at the sections of Injector, Linac section (L1, L2, L3, L4), bunch compressors (BC1, BC2, BC3), soft X-ray switch line, dechirper and deflector, emittance measurement unit (EMU), dogleg line, Undulator, and beam dump. The optics design also includes geometric and energy collimators to protect undulator magnets, whose performance is confirmed by the particle tracking simulation.

OUTLINE OF PAL-XFEL

The PAL-XFEL is designed to generate a 0.1 nm hard X-ray FEL using a 10 GeV electron linac with a switch line at 3 GeV point for soft X-ray FEL. The target slice emittance is 0.4 mm-mrad at 0.2 nC and the acceptable emittance is set at 0.6, which is used in the undulator design to have a reasonable margin of error [1].

Figure 1 depicts the layout of the PAL-XFEL. It consists of a 139-MeV injector, four acceleration sections (L1, L2, L3, and L4), three bunch compressors (BC1, BC2, BC3), and a dogleg transport line to undulators. The injector uses an S-band photo-cathode RF-gun to make the slice emittance smaller than 0.3 mm-mrad at 0.2 nC [2]. A laser heater, which placed right after the injector, is to mitigate micro-bunching instability by increasing the uncorrelated energy spread to Landau damp the instability. An X-band cavity placed after L1 is to linearize the non-linear energy-to-time correlation growing at the injector and L1 where the electron beam bunch is so long that non-linear time-varying RF field increases the non-linearity. A deflector, which is an RF cavity resonant at TM110 mode, is to measure the temporal profile of the electron beam and able to measure the energy-time correlation by incorporating with a following energy spectrometer. Emittance measurement unit (EMU) utilizes a FODO lattice with wire scanners placed between quads with a fixed betatron phase difference. A de-chirper located right after BC3-S in the soft X-ray FEL beamline is a corrugated pipe to actively use the resistive longitudinal wake field induced from the head of the bunch to decrease the energy of the tail. The energy chirp, time-correlated energy difference in the bunch, required in the bunch compression process is well compensated in the hard x-ray FEL beamline due to the long acceleration section

L4, while it is not available in the soft X-ray FEL beamline because there is no wake structure after the last bunch compressor (BC3-S). A 20-m long de-chirper is used in the soft X-ray FEL beamline while a short (6 m long) de-chirper will be used at the hard X-ray FEL beamline to have a possibility of increasing energy chirp, therefore, reducing R56, which means it allows us to reduce the amplitude of parameters affecting microbunching instability such as R56, chicane bend angle, and the distance between the first and the 2-nd dipole of chicane.

Figure 2 shows the layout of hard X-ray and soft X-ray FEL beamlines. Two FEL beamlines, one soft X-ray (SX1) and one hard X-ray (HX1), which will be prepared in the first phase, are to provide the FEL beam in the range of 0.56 to 0.1 nm and 4.5 to 1 nm, respectively. To have a capability of full polarization control in the soft x-ray FEL, APPLE-II type undulators are used for saturation at the last section of undulators before which planar-type undulators are used for full development of microbunching before saturation. The shortest wavelength of HX1 beamline is extendable to 0.06 nm by changing the undulator gap. The SX1 undulator line is nominally to deliver the FEL radiation from 3 nm to 1 nm, while it should be able to deliver a 4.5 nm FEL beam by reducing the beam energy from 3.15 to 2.6 GeV.

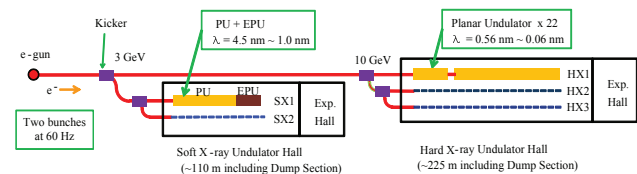


Figure 2: Layout of hard X-ray and soft X-ray FEL beamlines.

OPTICS DESIGN FOR HARD X-RAY FEL BEAMLINE

Hard X-ray FEL beamline

Figure 3 shows the lattice of the hard X-ray FEL beamline. Four acceleration sections (L1, L2, L3, and L4) have different FODO lattice with different betatron phases. The length of the S-band accelerating structure (A/C) is 3.0 meters. At L1, one quad per one A/C is selected to make betatron function smaller than 15 meters, and At L2 and L3, one quad per two A/Cs is selected to make betatron function smaller than 25 meters for L2 and 35 meters for L3. At L4, one quad per four A/Cs is selected because of small emittance of the electron beam.

* Work supported by Korean Ministry of Science and Technology

[†] hskang@postech.ac.kr

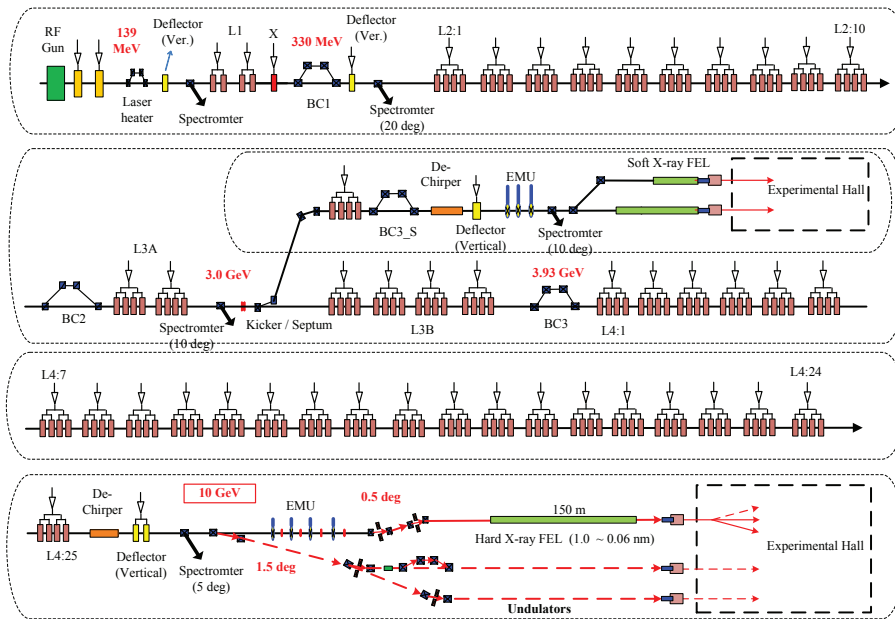


Figure 1: Layout of PAL-XFEL.

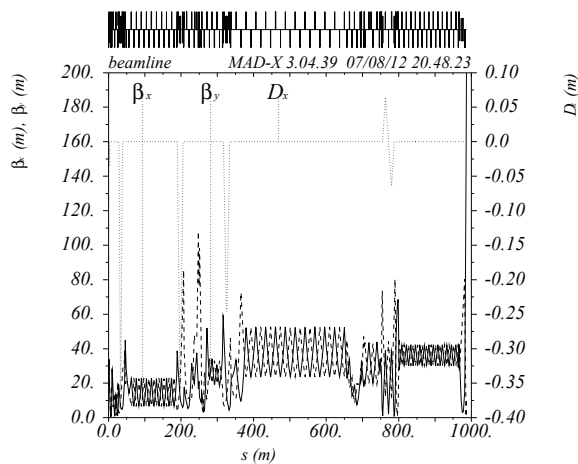


Figure 3: Lattice of hard X-ray FEL beamline.

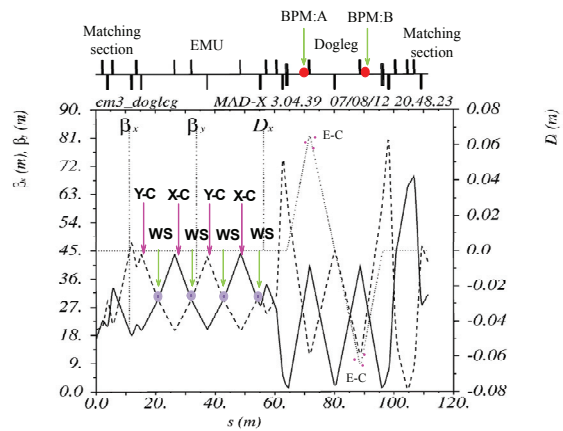


Figure 4: Lattice of emittance measurement unit and dogleg line. X-C and YC represent geometrical collimator, E-C energy collimator, and WS wire scanner.

Figure 4 shows the lattice of the emittance measurement unit (EMU) at the end of linac and a dogleg line to undulators where the beam energy is 10 GeV. EMU is a FODO lattice with phase advance of 45 degrees between quads with four wire scanners (WS) for emittance measurement placed mid between quads, where the betatron functions for both directions are same. Geometric collimators, horizontal (X-C) and vertical collimators (Y-C), are placed at two points for each direction with largest betatron function in the EMU. The phase difference between two collimators for each direction is designed to be 90 degrees.

The dogleg line consists of two dipoles with the bend angle of 0.5 degrees and three quads between dipoles. Dispersion at the quad is 0.063 m, which is large enough to provide a reading resolution of energy jitter for the BPM. Differentiating two x-BPM readings (BPM:A and BPM:B)

at the largest dispersive point cancel any betatron signal leaving only the energy signal. Energy jitter measurement resolution of $1E-5$ requires the BPM reading resolution of $0.6 \mu\text{m}$ at this BPM. Two energy collimators (E-C) are also placed at the point of largest dispersion in the dogleg line. Those collimators are to protect undulator magnet from misguided electrons and halo particles. The HX undulator chamber half gap of 2.6 mm and the maximum betatron function in undulator chain of 35 m give the required radius of 1.65 mm for geometric collimators in the EMU line. Clearance of the collimated beam in the undulator chamber is assumed to 20 % of the half gap, 0.52 mm. The required radius of energy collimator in dogleg line is 3 mm to cut out over $\pm 5\%$ energy electrons. The higher the

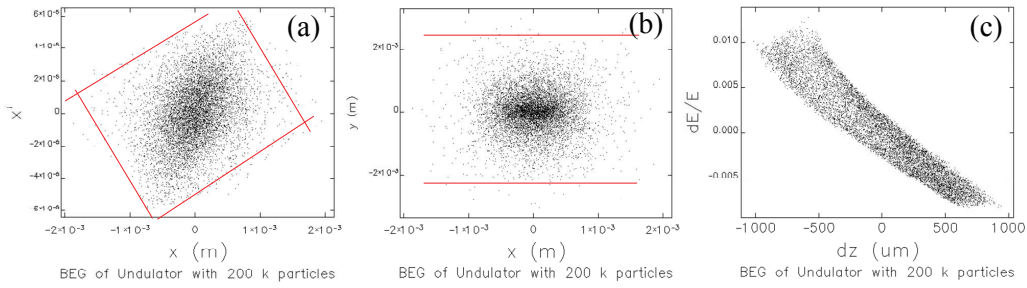


Figure 5: Particle tracking simulation for geometrical collimators and energy collimators: (a) horizontal phase space, (b) x-y distribution, and (c) energy bandwidth of the particle distribution at the undulator entrance.

betatron function in undulator chain, the bigger the radius of the geometric collimators in the EMU line.

Particle Tracking for Collimator

Particle tracking for the collimators above described is done using the elegant code [3]. A seed beam with 200k particles with an emittance of 100 mm-mrad and an energy spread ($\frac{\delta p}{p}$) of 0.1 starts from the exit of the injector. The input emittance is selected so as to clearly show the effect of collimator in the simulation. The center beam energy is 139 MeV and the bunch length is assumed 33 ps in rms. Four energy collimators (BC1-EC, BC2-EC, BC3-EC, HX-dogleg-EC) and two geometric collimators (HX-EMU:X-C, HX-EMU:Y-C) for each direction in the dog-leg line are tested in this simulation. The aperture radius of the energy collimator BC1-EC, BC2-EC, BC3-EC are 18.5 mm, 18 mm, 12 mm, respectively. It is clearly seen in Fig. 5(a) that two geometrical collimators with 90 degrees phase difference block halo particles to make the beam collimated defined by red line in the figure. The designed aperture of 1.65 mm for the geometric collimators gives a beam size of 2 mm at the entrance of the undulator ensuring that the simulation results match with the design value and the halo particle does not hit the undulator chamber. Figure 5(c) shows the energy bandwidth of the particle distribution, which reduces to 0.01 from the initial value of 0.1 by four energy collimators.

OPTICS DESIGN FOR SOFT X-RAY FEL BEAMLINE

Figure 6 shows the lattice of the SX FEL beamline and Figure 7 the lattice of dogleg switch line to soft X-ray FEL. The beam energy at the SX dog-leg line is 3 GeV. The SX dogleg line consists of two achromats whose dipoles have the bend angle of 3 degrees. Dispersion at the quad between two dipoles is 0.39 m, which is large enough to provide a reading resolution of 1E-5 energy jitter for the BPM (BPM:A and BPM:B). Geometric collimators (G-C), which is circular shape, are placed at two points between two achromatic bends. The phase difference between two geometric collimators is designed to be 90 degree in both directions. Two energy collimators (E-C) are also placed at

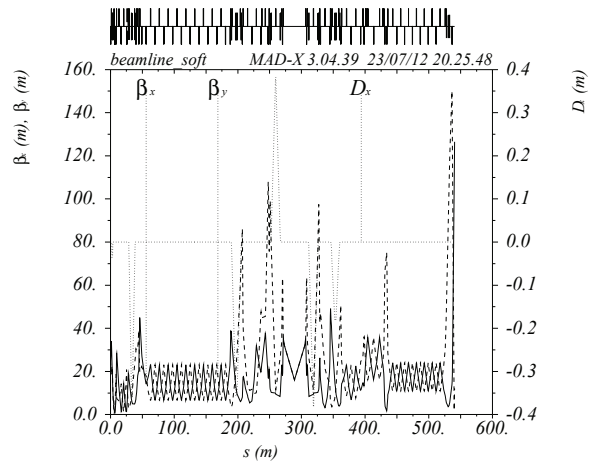


Figure 6: Lattice for Soft X-ray FEL beamline.

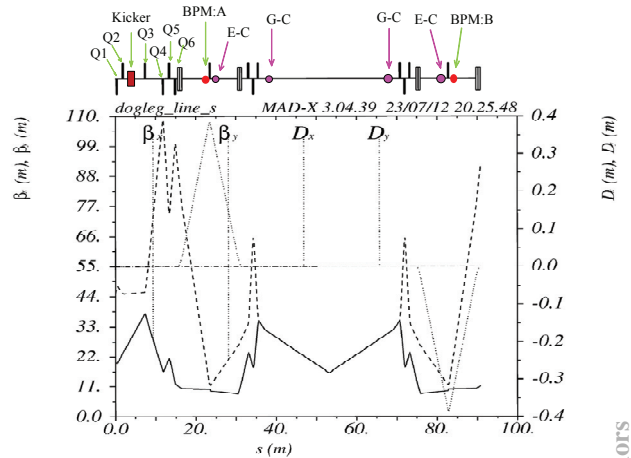


Figure 7: Lattice of dogleg switch line to soft X-ray FEL. G-C stands for geometrical collimator.

the point of largest dispersion in the SX dog-leg line. The SX undulator chamber half gap of 3.6 mm and the maximum betatron function in undulator chain of 24 meters give the required radius of 2.35 mm for geometric collimators in the SX dogleg line. The required radius of the energy collimator in the SX dogleg line is 19 mm to cut out over +/-5%

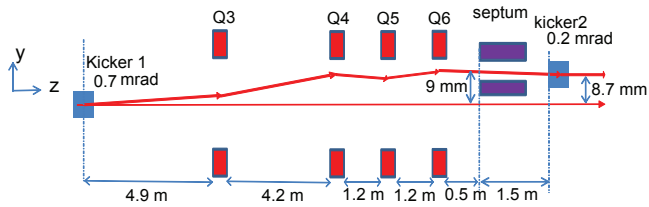


Figure 8: Beam offset along four quads to the septum. Q3, Q4, Q5, and Q6 are the same quads used in Fig. 7.

energy electrons.

A kicker and a septum are used for switching to soft X-ray FEL beamline. Electron beam is kicked vertically with the kick angle of 0.7 mrad at the kicker and then switched out horizontally at the septum where the vertical beam offset is 9.0 mm. Six quads are necessary for kick and matching to the SX dog-leg line. Q1 and Q2 are to make $\alpha_y = 0$ at the kicker, Q3 is to obtain an additional vertical kick, and Q4, Q5, and Q6 for matching to the dog-leg line contribute additional vertical kicks. Vertical dispersion appears along the dogleg switch line due to vertical kick, which can be removed by adding two vertical dipole correctors after the septum.

Beam offsets along four quads to the septum are depicted in Fig. 8. Four quads have different k-values to give different kick angles. After exiting Q6, the electron beam has the deflection angle of -0.2 mrad and a vertical offset of 9.0 mm at the entrance of the septum, which can be made parallel by the kicker-2 with the kick angle of 0.2 mrad.

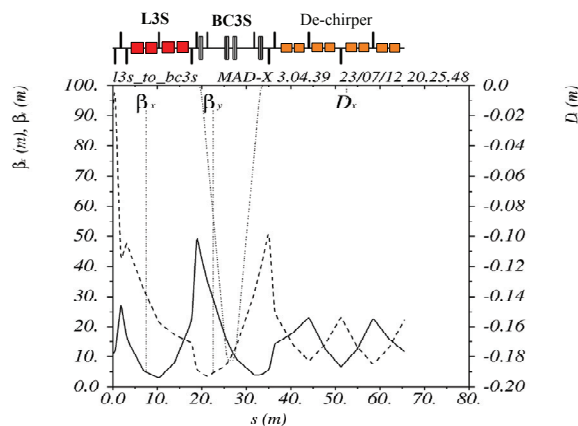


Figure 9: Lattice of L3S, BC3S, and De-chirper.

The lattice from L3S to De-chirper section is shown in Fig. 9. The beam energy is increased to 3.15 GeV at the L3S which consists of four S-band A/C powered by two klystrons. The horizontal betatron function is made smaller than 5 meters at the last dipole in BC3-S. The bend angle of chicane is variable from 0 to 2.2 degrees, which is also available in bunch compressors in the hard X-ray beamline. Two tweaker quads are placed at the separation of $\pi/2$ phase difference in the BC3-S. To reduce the effect of transverse wake field of the dechirper whose radius is as

ISBN 978-3-95450-123-6

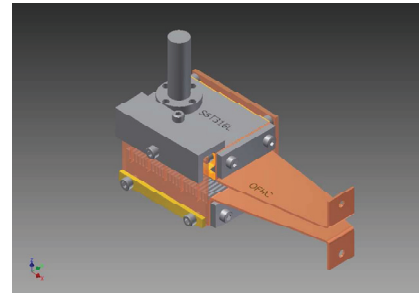


Figure 10: Entrance part of the 6-m long dechirper.

small as 3 mm, the betatron function around the dechirper is designed to be below 22 m. Figure 10 depicts the entrance part of the 6-m long dechirper which is now under design. It is an adjustable gap type of 5 to 30 mm using two parallel plates with corrugations to provide better controllability. But the wake reduces to a factor of $\frac{\pi^2}{16}$ from the circular type.

ROBUSTNESS OF THE LATTICE

The robustness of the lattice is simply tested with the input Twiss parameters varying by 50% from the design values (see Fig. 11). As seen in the figure, the optics distortion is not severe and the emittance increases by only a few percent. The distorted optics is easily recovered to the designed optics of Fig. 3 by re-matching of optics.

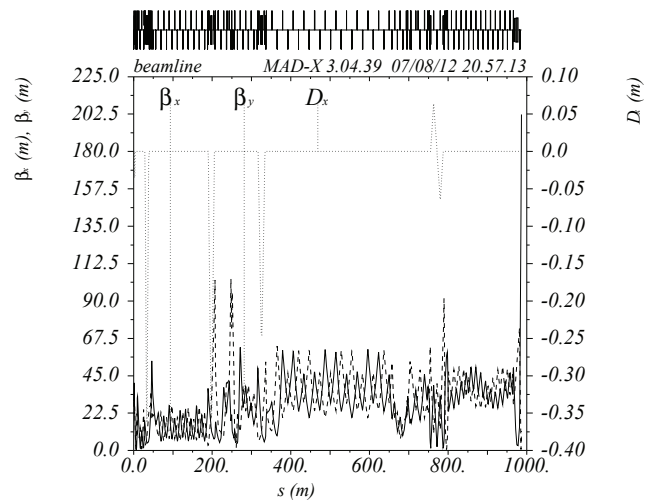


Figure 11: The lattice function with initial Twiss parameter varying by 50%.

REFERENCES

- [1] H. S. Kang et al., IPAC2012. p. 1738.
- [2] J.-H. Han et al., IPAC2012. p. 1772.
- [3] M. Borland, "Elegant: A Flexible SSD-Compliant Code for Accelerator Simulation".